Geophys. J. Int. (1996) **125**, 340–354

Glacial rebound of the British Isles—III. Constraints on mantle viscosity

Kurt Lambeck,[1] Paul Johnston,[1] Catherine Smither[1] and Masao Nakada[2]

[1]*Research School of Earth Sciences, The Australian National University, Canberra, ACT 0200, Australia*
[2]*Department of Earth and Planetary Sciences, Kyushu University, 33 Hakozaki, Fukuoka 812, Japan*

Accepted 1995 December 13. Received 1995 December 8; in original form 1995 April 7

SUMMARY

Observations of sea-level change since the time of the last glacial maximum provide important constraints on the response of the Earth to changes in surface loading on time-scales of 10^3–10^4 years. This response is conveniently described by an effective elastic lithospheric thickness and effective viscosities for one or more mantle layers. Considerable trade-off between the parameters describing these layers can occur, and different combinations can give rise to comparable predictions of sea-level change. In particular, the trade-off between lithospheric thickness and upper-mantle viscosity can be important, and for any reasonable value for the lithospheric thickness a corresponding mantle viscosity structure can be found that gives a plausible comparison of sea-level predictions with observations. In particular, thin-lithosphere models will lead to low estimates for the upper-mantle viscosity, while thick-lithosphere models lead to high viscosity values. However, either solution may represent only a local minimum in the model parameter space, and may not correspond to the optimum solution. It becomes important, therefore, that in the inversion of observational data, a comprehensive search is conducted throughout the entire model-parameter space, to ensure that the solution identified does indeed correspond to the optimum solution. The sea-level data for the British Isles lend themselves well to such an inversion because of the relatively high quality of the data, the good geographic distribution of the data relative to the former ice sheet, and reasonable observational constraints on the dimensions of the former ice sheet and on its retreat. Furthermore, because of the contribution to the sea-level signal from the distant ice sheets, as well as from the melt-water load, the observational data base for the region also has some resolving power for the viscosity of the deeper mantle. The parameter space explored is defined by up to five mantle layers, the lithosphere of effective elastic thickness D_1, and a series of upper-mantle layers, $i=2$–4, extending down to depths of 200, 400 and 670 km, respectively, each of viscosity η_i, and a lower-mantle layer of viscosity η_{lm} extending down to the core–mantle boundary. The range of parameters explored is $30 \le D_1 \le 120$ km, $3\times10^{19} \le \eta_i$ $(i=2, 3, 4) \le 5\times10^{21}$ Pa s, $10^{21} \le \eta_{lm} \le 10^{23}$ Pa s with $\eta_2 \le \eta_3 \le \eta_4 \le \eta_{lm}$. Simple models comprising three layers with $D_1 \sim 70$ km, $D_2 \sim 670$ km, $\eta_2 \sim (4$–$5)10^{20}$ Pa s, and $\eta_3 > 10^{22}$ Pa s describe the sea-level response to the glacial unloading well. Earth models with low-viscosity channels immediately beneath the lithosphere are not required, but if a thin lithosphere (< 50 km) is imposed in the inversion then the solution for the mantle viscosity leads to a low-viscosity ($< 10^{20}$ Pa s) channel. Such a model does not, however, represent the overall least variance solution that would be obtained if D_1 were also introduced as an unknown. Likewise, if a thick lithosphere (> 120 km) is imposed, then the solution points to a considerably higher value for the upper-mantle viscosity ($\sim 10^{21}$ Pa s). But this also represents only a local minimum solution. The observational data do point to some stratification in the viscosity of the upper mantle, and the optimum solution is for a five-layer model with the following effective parameters:

$55 < D_1 < 60$ km
$(2 < \eta_2 < 4) \times 10^{20}$ Pa s for $(D_1 < D \leq 200)$ km
$(4 < \eta_3 < 6) \times 10^{20}$ Pa s for $(200 < D \leq 400)$ km
$\eta_4 \sim 2 \times 10^{21}$ Pa s for $(400 < D \leq 670)$ km
$\eta_{lm} \gtrsim 10^{22}$ Pa s for $(670 < D < D_{cmb})$ km

Key words: British Isles, glacial rebound, mantle viscosity, sea-level.

1 INTRODUCTION

In two previous papers (Lambeck 1993a,b) (referred to hereafter as Parts I and II, respectively) the crustal rebound of Great Britain and the concomitant sea-level change associated with the melting of the last great ice sheets have been examined in detail, and models have been developed that relate mantle rheology and ice-sheet parameters to observations of relative sea-level change; i.e. the positions, in terms of both elevation and geographic location, of past sea-level with respect to its present position. These relations permit the viscosity of the mantle to be estimated, and also provide a basis for examining the evolution of the coastal and shallow-marine environment through Holocene and Late Pleistocene time (Lambeck 1995a). In these papers a comprehensive understanding of the relation between the past ice sheet over the region, sea-level change, and shoreline evolution has been reached, although some disagreements between observations and predictions that will require further improvements in certain aspects of the model have also been noted, most notably in the details of the ice sheet over northernmost Scotland and possibly over Ireland. While the models explain many of the observations well, the range of plausible earth models that describe the viscoelastic behaviour of the planet on time-scales of 10^3 to 10^4 years has not been fully explored. This arises because, under some conditions, different combinations of the earth-model parameters can give rise to similar predictions, and observations of sea-level change for the late- and postglacial stages may not give a unique determination of the parameters. It is this aspect of the problem that is discussed in this paper, in which a more comprehensive analysis of the model-parameter space has been carried out than has been the case previously. In order to compare the results with the earlier analyses, the same mathematical and physical models are used as described in Part II and Johnston (1993). The ice-sheet model and sea-level observational data base also remain unchanged and are not discussed further here.

The ice sheet over the Great Britain region was small compared with those over the former glaciated areas of Fennoscandia and Laurentia. But this small ice cap nevertheless produced significant crustal deflection whose record is well preserved in a range of now submerged or elevated shorelines around the coast and shallow off-shore areas. In addition to this local rebound, the past sea-levels of the region have also been influenced by the rebound of the crust under the weight of ice over Fennoscandia, as well as by the redistribution of meltwater into the surrounding oceans when the global ice sheets decayed. Thus, despite the relatively small extent of the former ice sheet, the sea-level data from the region contains some resolving power for the lower-mantle viscosity (below the 670 km seismic discontinuity), as well as considerable resolving power for the viscosity of the mantle above this boundary. This, coupled with a comprehensive data base of past sea-levels and a reasonable understanding of the retreat of the ice sheet since the time of the last glacial maximum, makes this region a valuable one for the study of glacial rebound.

The earth models used in modelling glacial rebound and the concomitant sea-level change are usually described by a series of concentric shells defined by realistically varying density and elastic parameters and depth-averaged effective viscosities. Typically the shells represent the lithosphere, with an effective elastic thickness D_1, one or more upper-mantle layers of viscosity η_2, η_3, ..., extending from the base of the lithosphere down to depths D_2, D_3, ..., and a lower mantle of effective viscosity η_{lm} from the 670 km seismic discontinuity down to the core–mantle boundary. The choice of these parameters in modelling the glacial rebound remains a matter for debate, thus values ranging from 30 km to 200 km have been used by different authors for the effective elastic thickness of the lithosphere (for a summary of lithospheric-thickness estimates see Wolf 1993). Fjeldskaar & Cathles (1992), for example, adopted the lower value throughout their modelling of the Fennoscandian rebound, while Peltier (1984, 1986) argued for values of 200 km from an analysis of the rebound of the Laurentide region, without fully examining the trade-off that may occur between this value and the mantle-viscosity parameters. Lambeck & Nakada (1990) and Lambeck, Johnston & Nakada (1990) found that intermediate values, of between 70 and 150 km, were more appropriate for most glacial-rebound and sea-level modelling, and that the actual value obtained was closely related to the estimates of the mantle viscosity. Nor has there been much agreement on the inferences of the viscosity of the mantle from the rebound and sea-level studies. Thus Fjeldskaar (1994) argued for a low-viscosity channel immediately below the lithosphere with an effective viscosity of 2×10^{19} Pa s, whereas Peltier and colleagues argued for a nearly uniform mantle viscosity of 10^{21} Pa s from the base of the lithosphere down to the core–mantle boundary (e.g. Peltier, Drummond & Tushingham 1986), although in their more recent models the viscosity of the lower mantle has increased somewhat (Peltier & Tushingham 1991; Mitrovica & Peltier 1993). In contrast, Nakada & Lambeck (1989) argued that the lower-mantle viscosity is distinctly greater than that of the average upper mantle, a view recently supported by Mitrovica, Davis & Johansson (1995).

For a large part, these differences in the inferred parameters are a consequence of the trade-off that occurs between the parameters describing the mantle structure, and by an inadequate search through the model-parameter space. Only the studies of Nakada & Lambeck (1989) [see also Lambeck & Nakada (1990); Lambeck *et al.* (1990); Part II] have attempted

to search over a wide range of lithospheric-thickness and mantle-viscosity parameters, and even these studies have not covered the entire plausible range. This paper sets out to rectify this limitation, as well as to illustrate some of the consequences of not conducting a full search through the model parameter space.

The observation equation used to estimate the effective viscosity of the mantle and the lithospheric thickness, as well as other pertinent model parameters, is given by eq. (1) of Part II, and this is written here as

$$\Delta\zeta_0(\varphi,t)+\varepsilon_0(\varphi,t)=\Delta\zeta^{\,e}(t)+\delta\zeta^{\,e}(t) +\beta\Delta\zeta^{\,BR}(\varphi,t)+\Delta\zeta^{\,f-f}(\varphi,t)+\Delta\zeta^{w} =\Delta\zeta_{\text{predicted}}, \quad (1)$$

where

$\Delta\zeta_0$ is the observed sea-level, reduced to mean sea-level, at location φ and time t (see Part II);

ε_0 is the assumed observation error (see Part II);

$\Delta\zeta^e$ is the eustatic sea-level function for the combined ice sheets;

$\delta\zeta^{\,e}$ is the correction term to $\Delta\zeta^e$;

β is the scale parameter for the British ice sheet;

$\Delta\zeta^{BR}$ is the predicted first-iteration isostatic contribution to sea-level change from the ice- and water-load of the British ice sheet for specified earth-model parameters; it also includes the contribution arising from the change in gravity field;

$\Delta\zeta^{f-f}$ is the predicted isostatic and gravitational contribution from the more distant (far-field) ice sheets of Fennoscandia, Laurentia, Barents-Kara, and Antarctica;

$\Delta\zeta^{w}$ is the second-iteration correction to the water-load terms resulting from (1) the dependence of the water-load term on sea-level change itself, and (2) the time dependence of the shoreline locations.

Generally the heights of the ice sheets are poorly constrained by direct observational evidence and are instead based on indirect considerations. For this reason, the scale parameter β has been introduced into the observation equation (1), although, for the British Isles, the ice heights are partly constrained by evidence of trim-lines near the peaks of some of the higher mountains that stood out as nunataks, and this information has been incorporated into the ice model used here (Part II). As before, an iterative procedure has been adopted to solve for the earth-model parameters (D_j, η_j of the j layer model), which are embedded directly in the isostatic functions $\Delta\zeta^{\,BR}$ and $\Delta\zeta^{f-f}$, the ice-height scale parameter β, and the corrective term to the eustatic sea-level function $\delta\zeta^{\,e}$.

The degree of fit of the predictions of a particular earth model, k, to the observations is defined by the variance function (eq. 2 of Part II) as

$$\Psi_k=\frac{1}{M}\sum_{m=1}^{M}\left[\frac{\Delta\zeta_0^m-\Delta\zeta_{\text{predicted}}^m}{\sigma^m}\right]^2, \quad (2)$$

where $M=424$ is the total number of observations, each with standard deviation σ^m.

A systematic model-parameter search is conducted for

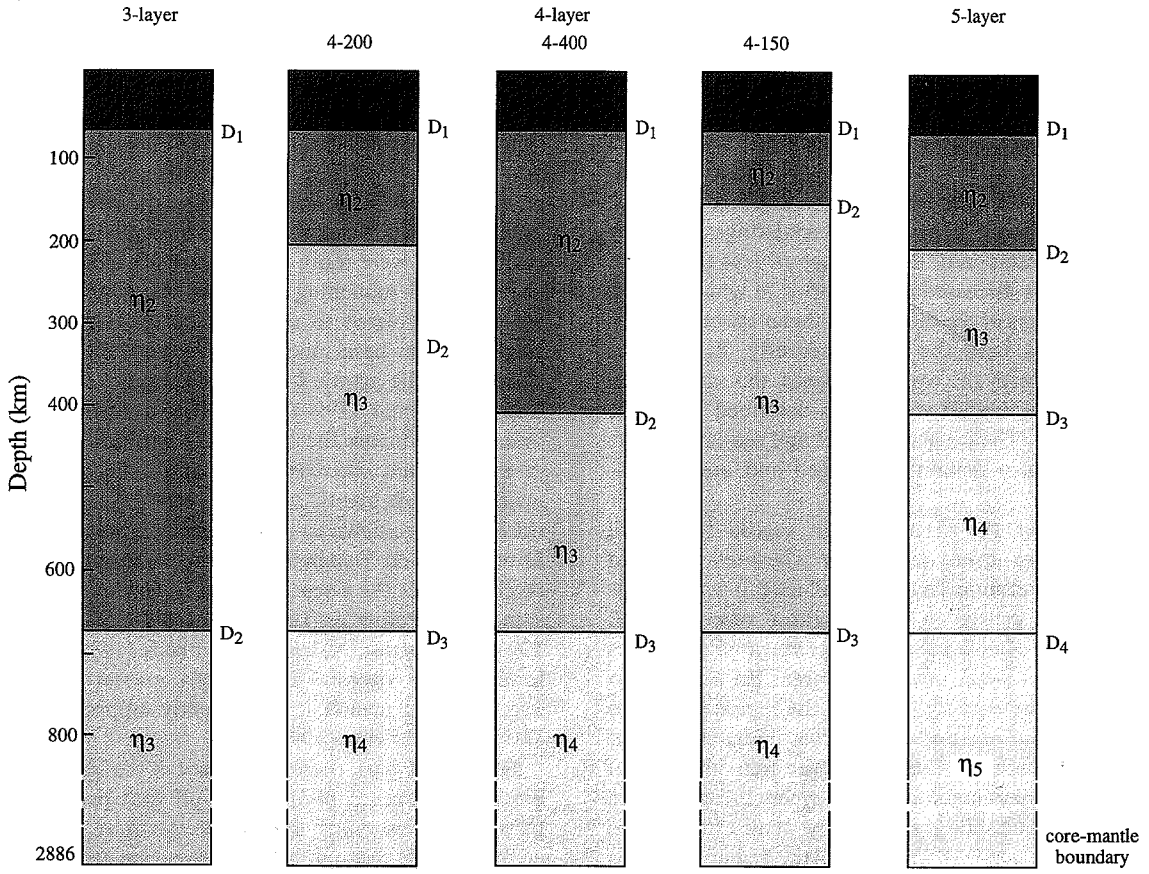

Figure 1. Summary of the zonation of the viscosity structure of the mantle for the three-, four- and five-layer models. Elastic moduli and density depth profiles are derived from seismic models of the mantle, in this case the PREM model of Dziewonski & Anderson (1981).

different classes of models, which are defined by the number of shells in the mantle model. For each set of earth-model parameters in this space, the β parameter (as well as, in the higher-iteration solutions, the eustatic sea-level corrective term) that gives the best least-squares fit to the observational data for that particular earth model is estimated. The overall minimum variance is then found by searching through a range of plausible earth-model parameters, $k=1,\ldots,K$, that is sufficiently large to ensure that the global minimum-variance solution, rather than simply some local minimum variance, is found.

2 THREE-LAYER MODELS

A first-order zonation of the mantle is in terms of three layers (Fig. 1): an effectively elastic lithosphere of thickness D_1, an upper mantle of viscosity η_2 extending from the base of the lithosphere down to the major seismic discontinuity at $D_2=$ 670 km depth, and a lower mantle extending from 670 km depth down to the core–mantle boundary at depth $D_{\rm cmb}=$ 2891 km. The parameter space within which a solution for the three-layer mantle structure is sought is defined by $30\leq D_1\leq 120$ km, $10^{20}\leq\eta_2\leq 10^{21}$ Pa s, $10^{21}\leq\eta_{\rm lm}\leq 10^{23}$ Pa s, although in some of the subsequent model classes, lower values for η_2 will be examined. Fig. 2 illustrates the dependence of the variance factor ψ_k (eq. 2) on the two viscosity values for some discrete values of D_1. These results are for the first-iteration solutions, in which the meltwater load is approximated by the eustatic sea-level change, and do not include the eustatic correction term. For all values of D_1 examined (Table 1), the most obvious result is the strong contrast between the two viscosities η_2 and $\eta_{\rm lm}$. While the resolution for the lower-mantle viscosity itself is not strong, the results require that the lower-mantle viscosity is of the order 10^{22} Pa s and that it exceeds that of the upper-mantle layer by a factor of as much as 50, depending on the lithospheric thickness adopted.

As discussed briefly above, the resolving power for the lower mantle comes largely from the far-field isostatic corrections, including the water-load term. Fig. 3 illustrates this in the form of the ratio

$$\Gamma=\left\{\frac{\sum_m\left[\sum_{j*}\delta\zeta^{j*}\right]^2}{\sum_m\left[\sum_j\delta\zeta^{j}\right]^2}\right\}^{1/2}. \qquad (3)$$

$\delta\zeta$ refers to the departures of the predicted sea-level from the eustatic approximation for ice sheet j. The summation j is over the totality of the ice sheets (with $\beta=1$), and the summation j^* is over all the ice sheets except the British Isles. The summation m is, as in eq. (2), over all 424 observation locations and times contributing to the solution of the observation equation. The results for Γ in Fig. 3 are for $D_1=65$ km, and the contribution from the far-field ice sheets of Fennoscandia, Laurentia and Antarctica to the total sea-level signal varies, according to earth model, from about 10 to 20 per cent. For $D_1=50$ km this contribution is smaller, and less model-dependent, being of the order of 8 to 12 per cent. For larger D_1 values the contribution is both larger and more strongly model-dependent, ranging from about 15–25 per cent for

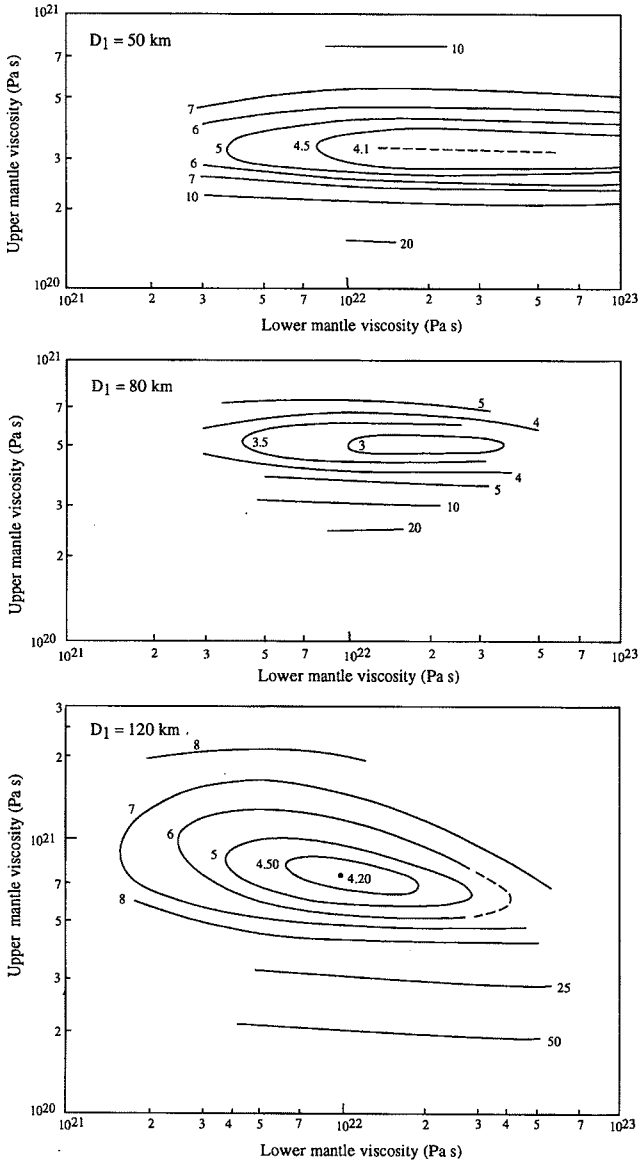

Figure 2. Minimum-variance function Ψ_k for the three-layer models for $D_1=50$, 80, and 120 km, and variable upper- and lower-mantle viscosities.

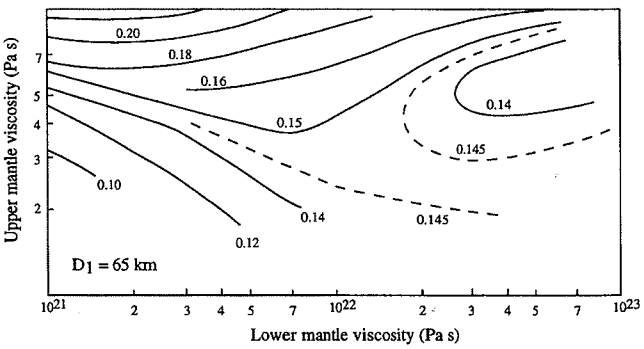

Figure 3. Ratio of the far-field to total contributions to the sea-level change at times and locations of observations, the function Γ defined by eq. (3), as a function of η_2 and $\eta_{\rm lm}$ for $D_1=65$ km.

Table 1. Summary of first-iteration three-layer model solutions for specific values of the lithospheric thickness D_1 and second-iteration solutions with and without the corrective term $\delta\zeta^e$ for the eustatic sea-level function. For the second-iteration solutions only models with $\eta_{lm}=1.3\times10^{22}$ have been considered. (Units for all viscosities are Pa s).

	D_1	η_2	η_{lm}	β	Ψ
1st - iteration	50	$3.3\text{x}10^{20}$	$\geq10^{22}$	0.90	4.10
	65	$4.2\text{x}10^{20}$	$\geq10^{22}$	1.06	2.75
	80	$5.0\text{x}10^{20}$	$\geq10^{22}$	1.24	2.95
	100	$6.0\text{x}10^{20}$	$\geq10^{22}$	1.44	3.74
	120	$7.5\text{x}10^{20}$	$\simeq10^{22}$	1.87	4.26
2nd - iteration (excl. $\delta\zeta^e$)	70	$(4\text{-}5)10^{20}$	$1.3\text{x}10^{22}$	1.06	2.50
2nd - iteration (incl. $\delta\zeta^e$)	(65-70)	$(4\text{-}5)10^{20}$	$1.3\text{x}10^{22}$	1.04	1.90

$D_1=80$. These results indicate that these far-field contributions to the total sea-level predictions are significant, ranging from 10 to 25 per cent, and that they do exhibit some dependence on the lower-mantle viscosity, which permits some separation of values for the upper and lower mantle.

The results illustrated in Fig. 2, as well as similar results for intermediate values of D_1, suggest that the effective viscosity of the lower mantle is of the order of 10^{22} Pa s or possibly somewhat higher but a better resolution for this parameter from this data base is not achievable. Instead, analyses similar to the present one will be required for some of the larger Late Pleistocene ice sheets. Some trade-off between the other two parameters, D_1 and η_2, is also evident. For example, if only models with a 50 km thick lithosphere are considered then the optimum solution, defined as the minimum value for Ψ_k for models with $D_1=50$ km, yields $\eta_2\sim3\times10^{20}$ Pa s. If an *a priori* value of $D_1=120$ km is adopted then $\eta_2\sim7\times10^{20}$ Pa s, but both solutions would only be local minima (see Fig. 5(a) below). Thus, models with a thick lithosphere lead to a relatively high estimate for the upper-mantle viscosity, whereas models with a low D_1 lead to a smaller value for η_2. This result may at first be counter-intuitive, but it arises from the fact that often sea-level observations are available for only the latter part of the time span since the initiation of melting of the ice sheet. Consider the expected sea-level change at a locality near the centre of the ice sheet. For a given D_1, models with a low viscosity give a large overall relative sea-level change when viewed at a time t' sometime after the removal of the ice load, and the relative sea-level curve will be characterized by a rapid, nearly exponential change [curve i, Fig. 4]. In contrast, models with the same D_1 but a high upper-mantle viscosity give a smaller amount of relaxation by the time t', but the sea-level curve will be characterized by a more uniform decay (curve ii). For models with a thicker lithosphere the relative behaviour for low (curve iii) and high (curve iv) mantle viscosities is similar, but the overall amplitudes will be reduced. Thus, for a given amount of observed sea-level change in an

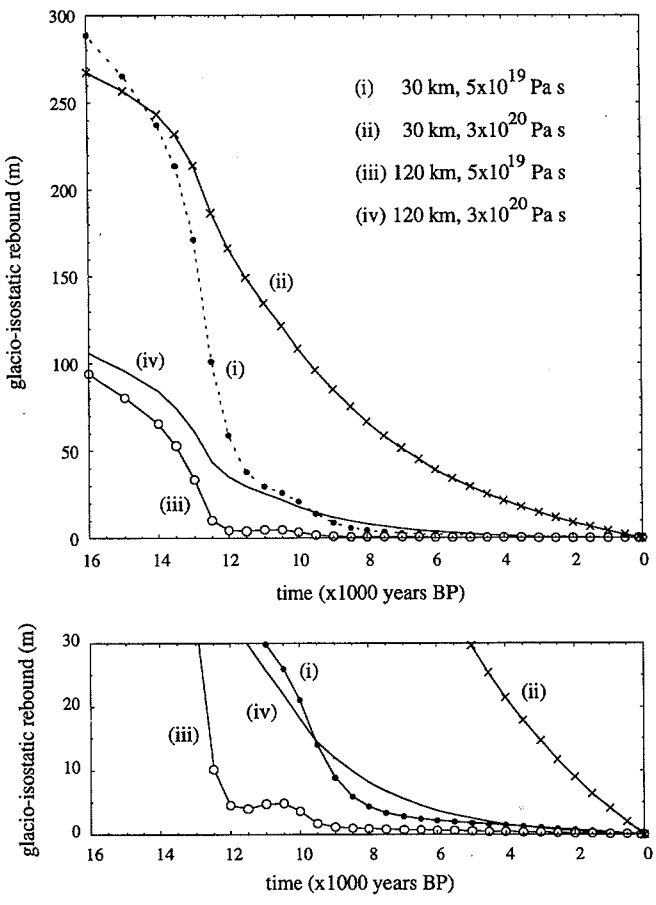

Figure 4. Glacio-isostatic rebound near the centre of the ice load over Scotland for four different earth models. If observations are reliable for only the last 11 000 a, model (i) (thin lithosphere, low upper-mantle viscosity) gives a similar prediction to model (iv) (thick lithosphere, higher upper-mantle viscosity). The lower panel gives the same results, but for an expanded height scale.

interval corresponding to the postglacial phase, about the last 10 000 a in this case, it may become difficult to distinguish between a model with (1) an initially large displacement (small D_1) and rapid relaxation (small η_2) (curve i), and (2) a smaller initial displacement (large D_1) with a slower relaxation (large η_2) (curve iv). Usually few observations are available from sites near the centre of the former ice sheet, but this argument is also valid for sites near and beyond the former ice-sheet margins. Thus the effective separation of the two parameters requires high-quality observations that constrain the curvature of the sea-level time-series, observations that extend as far back in time as possible, and observations from localities at varying distances from the centre of the former ice sheet. The attraction of the British ice sheet for glacial-rebound modelling is that it meets these criteria well.

Fig. 5(a) illustrates the variance plots for the D_1–η_2 space for models with a lower-mantle viscosity η_{lm} of 1.3×10^{22} Pa s. Other values for η_{lm} give similar locations for the minimum variance. This result clearly shows the importance of searching through a wide domain of model parameters, and that the prior assumption of a value for D_1 can lead to solutions that represent only local minima.

The results in Fig. 5(a) are for the first-iteration solutions in which the ice-height scale parameter has been included as an unknown. That the β value for the minimum-variance solution lies close to unity suggests that the use of the trim-line evidence to constrain the ice heights leads to a satisfactory estimate of the ice thickness during the glacial maximum stage. Some trade-off between the earth-model parameters and this scale parameter can occur, with thick-lithosphere models requiring more ice in order to match a given amount of rebound, and this could be used to place some constraint on the range of plausible solutions. Thus, models based on a lithosphere of 120 km thickness, for example, require a maximum thickness of the ice sheet that is about 80–90 per cent greater than inferred from the geomorphological evidence. The required maximum ice height at the time of peak glaciation in this case would be about 2600 m, compared with about 1500 m for the solution corresponding to the overall minimum variance, and quite inconsistent with the trim-line evidence, as well as

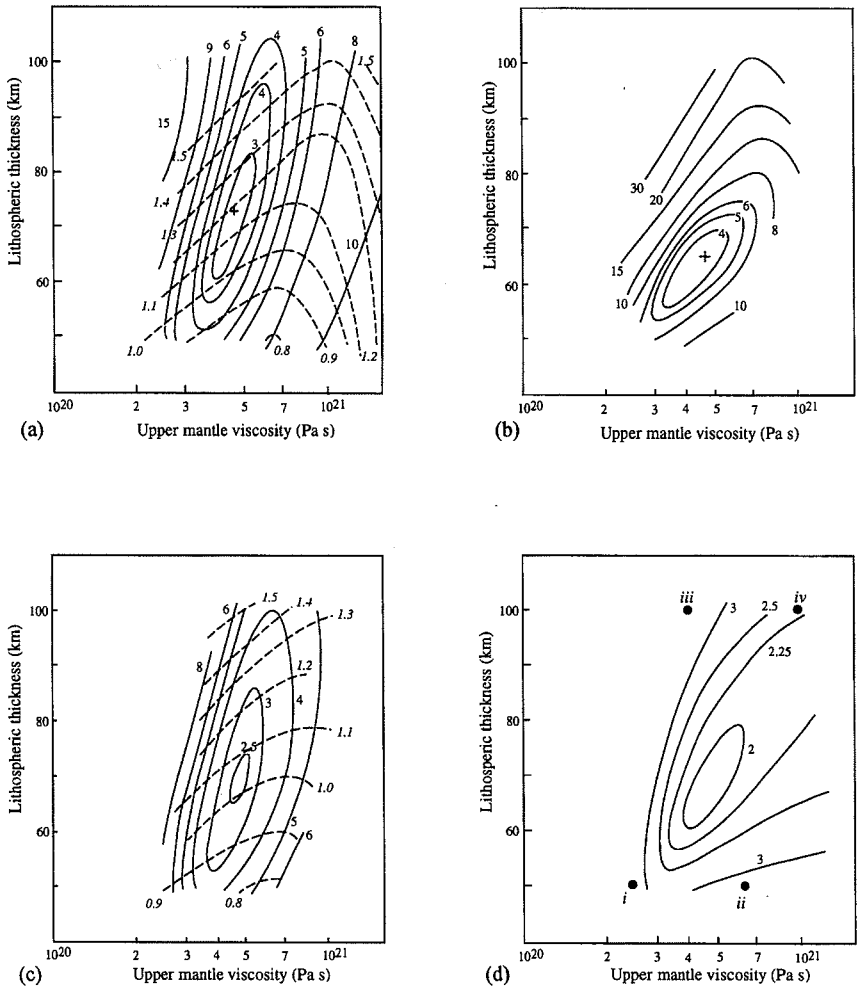

Figure 5. Minimum-variance function Ψ_k for the three-layer models with $\eta_{lm} = 1.3 \times 10^{22}$ Pa s. (a) First-iteration solution, including solving for the β parameter. The continuous lines indicate contours of minimum variance and the cross locates the global minimum. The dashed lines indicate contours of the β parameter (values in italics). (b) Ψ_k for the first-iteration solution in which the β parameter is set to 1. (c) Ψ_k for the second-iteration solution, including the water-load corrective term $\Delta\zeta^w$, but excluding the eustatic corrective term. Dashed curves indicate contours of constant β. (d) Second-iteration solutions including the corrective term to the eustatic sea-level function. Points marked *i* to *iv* refer to the models whose eustatic correction terms are illustrated in Fig. 6(a).

implausible from ice-modelling considerations (e.g. Boulton, Smith & Morland 1984; Boulton *et al.* 1985). Thin-lithosphere models will, in contrast, lead to an underestimation of the ice volume (Fig. 5a), and the maximum ice-height estimate for the 30 km model is about 1000 m. If ice thicknesses were known from independent observational data then solutions with $\beta=1$ would be appropriate, and Fig. 5(b) illustrates results based on this assumption. The minimum variance occurs for the same parameters as before, but the results do illustrate the advantage of independent constraints on the ice height, in that the separation of the two parameters is considerably improved because of the elimination of the correlation of the parameters with β. Whether or not β is introduced as an unknown in the observation equation also affects the solutions carried out within restricted ranges of earth-model parameters. For example, by setting β to unity, implying that the ice sheet is fully known from *a priori* information, solutions with an imposed thick lithosphere result in a higher upper-mantle viscosity than if β is introduced as an unknown. Compare, for example, the location of the minimum global variances in Figs 5(a) and (b). Likewise, the effect of holding β constant when imposing a thin lithosphere on the mantle model is to reduce the estimate of the viscosity of the underlying layer.

Fig. 5(c) illustrates results that are comparable to those illustrated in Fig. 5(a), except that the second-iteration corrections for the water-load term, including the time-dependent migration of shorelines, has been included, using the formulation discussed by Johnston (1993). The effect of the second iteration, at least for these three-layer models, is to reduce the value of the overall minimum variance with negligible consequence on the earth-model parameters themselves. Hence, for a preliminary exploration of the model space it does not appear to be necessary to consider these second (and higher) iterations of the sea-level equation.

The first-iteration solution is based on a eustatic sea-level curve that has been estimated from observations, corrected for isostatic effects, from sites that lie far from the former ice sheets, and where the primary contribution to sea-level is the eustatic change. The nominal curve used here is characterized by a smoothly varying function in which all melting ceased at 6000 a BP. Earlier work on Holocene sea-levels in the far-field has led to the conclusion that some modification of this eustatic sea-level function is appropriate, in particular that the ocean volumes may have increased slightly after about 6000 a BP (Nakada & Lambeck 1988) and modifications before this time may also be warranted (see Part II; Lambeck *et al.* 1990). The complete solution should also include, therefore, the corrective term for the eustatic sea-level function. The minimum-variance functions for such solutions are illustrated in Fig. 5(d). The principal consequence of the inclusion of the eustatic correction term is that the overall variances are reduced throughout the model space explored but that the minimum occurs for the same earth-model parameters as before (Table 1). The correlation between this correction and the other parameters is most pronounced with viscosity, with low and high upper-mantle viscosity models giving large corrections for late-glacial time (Fig. 6a), but of opposite sign. These extreme corrections appear to be inconsistent with the sea-level evidence from sites far from the former ice margins, but further work on estimating the eustatic sea-level function from such far-field data is desirable, in particular as these estimates for the oldest ages are based on only a few data points. The corrective terms for

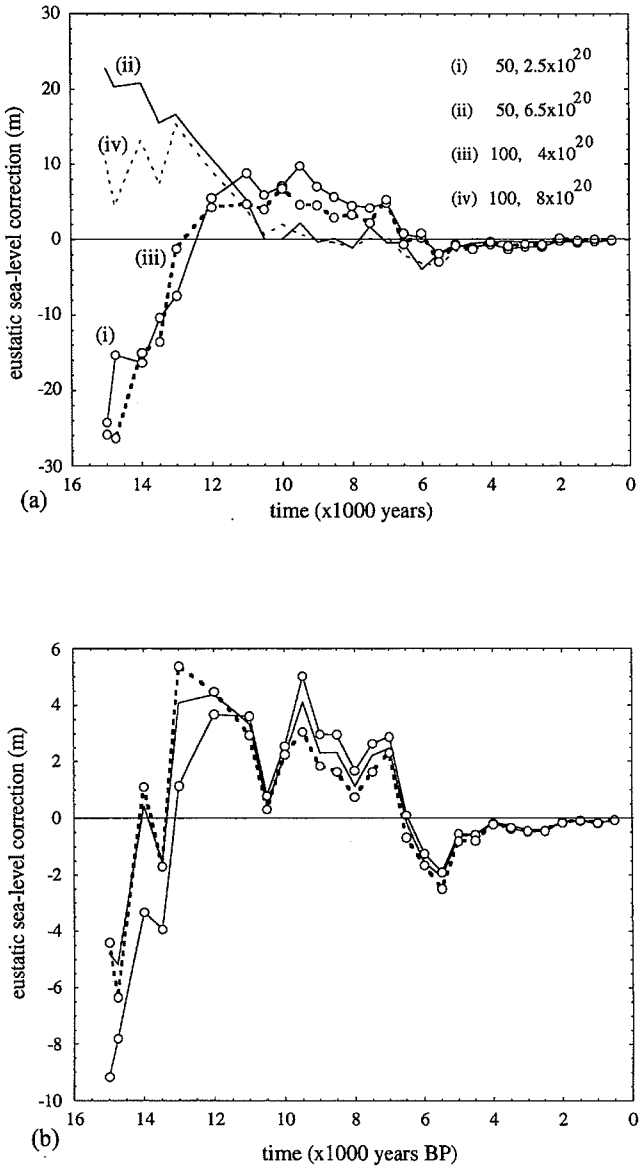

Figure 6. (a) Estimates for the second-iteration corrective term to the eustatic sea-level function for two models with (i, ii) a relatively thin lithosphere (50 km), (iii, iv) a relatively thick lithosphere (100 km). Models (i) and (iii) have relatively low upper-mantle viscosities and models (ii) and (iv) have higher viscosities. (See Fig. 5d for the location of these solutions in the D_1–η_{um} space.) (b) The eustatic correction for three models near the minimum-variance solution (within the $\Psi=2$ contour of Fig. 5d).

the models near the overall minimum variance yield much smaller corrections (Fig. 6b) and are consistent with the earlier conclusions of Nakada & Lambeck (1988) that ocean volumes have increased since about 6000 a ago, such as to raise the eustatic sea-level by about 2 m.

The amplitude of the minimum-variance function obtained for the most comprehensive of the three-layer models is about 2, compared with an expected value of unity if the model is complete and the standard deviation estimates adopted for the observations are true reflections of their accuracy. The observational accuracies have been previously discussed (Part II) and are considered to be conservative, so that the minimum value obtained for Ψ_k suggests that there may be some scope

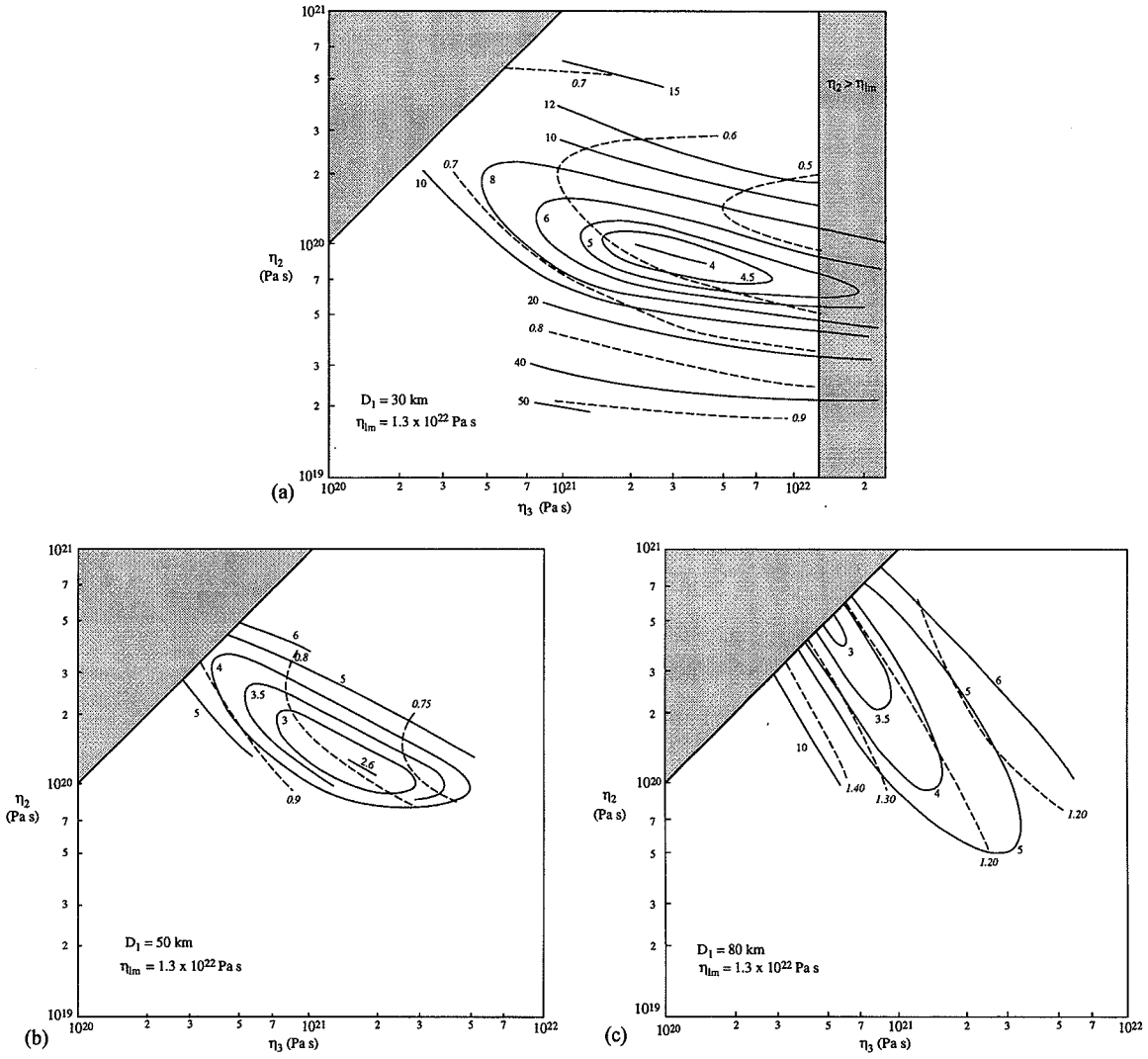

Figure 7. Minimum-variance functions for four-layer models with $D_2 = 200$ km and $\eta_{lm} = 1.3 \times 10^{22}$ Pa s. (a) $D_1 = 30$ km; (b) $D_1 = 50$ km; (c) $D_1 = 80$ km.

for further model improvement. Furthermore, the results so far do not address the question whether the observational data requires the introduction of a low-viscosity zone, as suggested by Fjeldskaar & Cathles (1992) and Fjeldskaar (1994). Such models are examined below.

3 FOUR-LAYER MODELS

Suggestions that the glacial rebound data require the existence of a low-viscosity channel go back to the important works by Daly (1934), van Bemmelen & Berlage (1935) and Cathles (1975), and have been most recently supported by the detailed work of Fjeldskaar (1994) (see also Fjeldskaar & Cathles 1992). To examine whether the British data warrant such a structure, the above procedures have also been applied to a four-layered earth model in which layer 2 (of viscosity η_2) extends from the base of the lithosphere to a depth of 200 km below the surface (Fig. 1). The third layer (of viscosity η_3) extends from 200 km down to the 670 km discontinuity and the fourth layer (of viscosity η_{lm}) is the lower mantle between 670 km and the core–mantle boundary. The three-layer model results indicated that resolving power for the viscosity of this last layer is unlikely to be high, and the previously determined value of $\eta_{lm} = 1.3 \times 10^{22}$ Pa s is adopted in the first instance. The search through the model space for the remaining parameters is then $30 \leq D_1 \leq 80$ km, $10^{19} \leq \eta_2 \leq 10^{21}$ Pa s, $10^{20} \leq \eta_3 \leq 10^{22}$ Pa s, with $\eta_2 \leq \eta_3 \leq \eta_{lm}$. Only first-iteration solutions will be considered initially. Fig. 7 illustrates the minimum-variance function in the η_2–η_3 domain for three values of D_1. A single local minimum is found in each instance, and for any value of lithospheric thickness a well-defined solution for both η_2 and η_3 follows, although η_2 is generally better determined. For $D_1 = 30$ km (Fig. 7a) the solution points to a well-defined low-viscosity channel. Thus, if the lithospheric thickness is assumed to have a value of 30 km then the conclusion would be drawn that there is a low-viscosity zone immediately below the lithosphere. However, the minimum variance obtained in this case is not the overall smallest value when different values for D_1 are considered. For 50 km, for example (Fig. 7b), the overall minimum variance is significantly reduced (Table 2).

Table 2. Summary of solutions for the four-layer models. (a) $D_2=200$ km for two different values of η_{lm}, (b) $D_2=400$ km, (c) $D_2=150$ km, for specified values of lithospheric thickness D_1 and lower-mantle viscosity (units for all viscosities are Pa s).

	D_2 (km)	D_1 (km)	η_2	η_3	η_{lm}	β	Ψ	Iteration
(a)	200	30	9×10^{19}	2.8×10^{21}	1.3×10^{22}	0.56	4.00	1
		50	1.3×10^{20}	1.3×10^{21}	1.3×10^{22}	0.76	2.65	1
		65	2.5×10^{20}	6×10^{20}	1.3×10^{22}	1.00	2.85	1
		80	5×10^{20}	5×10^{20}	1.3×10^{22}	1.25	2.95	1
(a)	200	30	1.0×10^{20}	3×10^{21}	0.5×10^{22}	0.58	4.70	1
		50	1.1×10^{20}	2.5×10^{21}	0.5×10^{22}	0.82	3.00	1
		80	5×10^{20}	5×10^{20}	0.5×10^{22}	1.28	3.32	1
(b)	400	50	3×10^{20}	2.5×10^{21}	1.3×10^{22}	0.76	2.50	1
		65	3.3×10^{20}	2.0×10^{21}	1.3×10^{22}	0.92	2.35	1
		65	3.7×10^{20}	1.5×10^{21}	1.3×10^{22}	0.91	2.21	2
		80	4.2×10^{20}	1.2×10^{21}	1.3×10^{22}	1.17	2.80	1
(c)	150	30	5×10^{19}	2×10^{21}	1.3×10^{22}	0.61	3.72	1

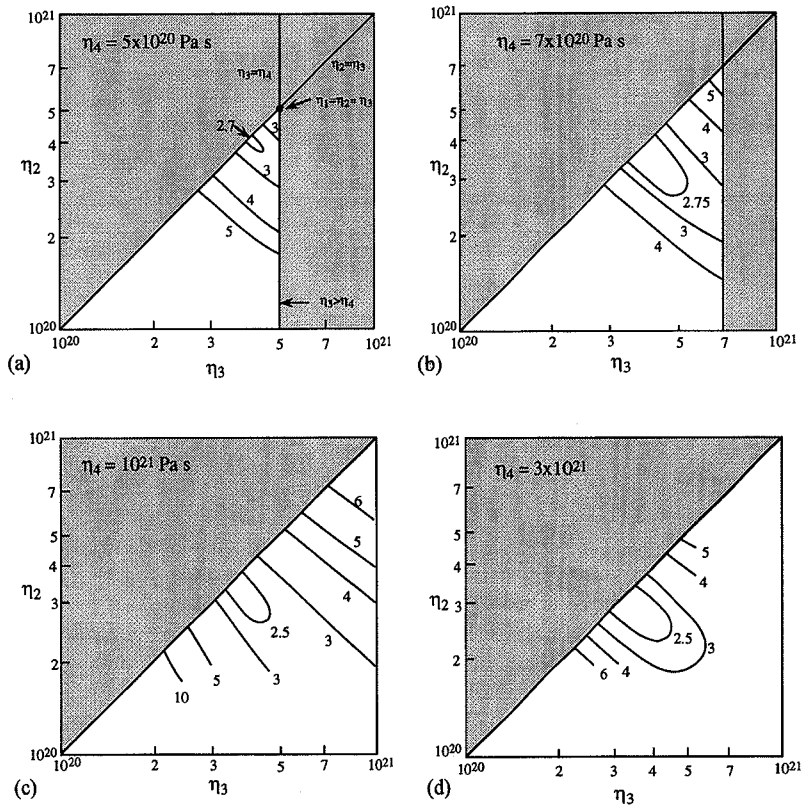

Figure 8. Minimum-variance functions for five-layer models. $\eta_{lm}=1.3\times10^{22}$ Pa s, $D_1=65$ km, and selected values for the viscosity η_4 of the transition zone. (a) $\eta_4=5\times10^{20}$, (b) 7×10^{20}, (c) 10^{21}, (d) 2×10^{21}. Only models in which $\eta_2<\eta_3<\eta_4<\eta_{lm}$ are considered, with $D_2=200$ km, $D_3=400$ km and $D_4=670$ km.

Table 3. Summary of solutions for first-iteration five-layer models for specified values of the lithospheric thickness D_1 and the second-iteration solution not including the correction term for the eustatic sea-level function. All lower-mantle viscosities are set to 1.3×10^{22} Pa s. The last solution is for the modified British ice sheet (see text) and includes the correction for the eustatic sea-level function.

	D_1	η_2	η_3	η_4	β	Ψ
1st iteration	30[1]	10^{20}	2×10^{21}	2×10^{21}	0.58	4.04
	50	1.4×10^{20}	7×10^{20}	2.5×10^{21}	0.77	2.40
	57.5	2.8×10^{20}	3.1×10^{20}	2.5×10^{21}[2]	0.84	2.16
	65	3.3×10^{20}	3.3×10^{20}	2×10^{21}	0.92	2.35
	80	4.2×10^{20}	4.2×10^{20}	1.2×10^{21}	1.17	2.84
2nd iteration	50[2]	1.4×10^{20}	10^{21}	2.5×10^{21}	0.74	2.15
	57.5[2]	2.2×10^{20}	5×10^{20}	2.5×10^{21}	0.81	2.10
	65	3.5×10^{20}	3.5×10^{20}	2×10^{21}	0.89	2.27
	80[3]	4.5×10^{20}	4.5×10^{20}	10^{21}	1.11	2.80
2nd iteration	57.5	2×10^{20}	6×10^{20}	2.5×10^{21}	0.80	1.35

[1] The search through η_2 and η_3 was carried out for $D_1 = 30$ km with η_3 set to 2×10^{21} Pa s, based on the values obtained for the other models for which the search through the η_4 dimension was more comprehensive.
[2] The search at these values of D_1 was conducted through η_2–η_3 space only, with η_4 set to 2.5×10^{21} Pa s.
[3] Models with $\eta_4 = 10^{21}$ Pa s only considered.

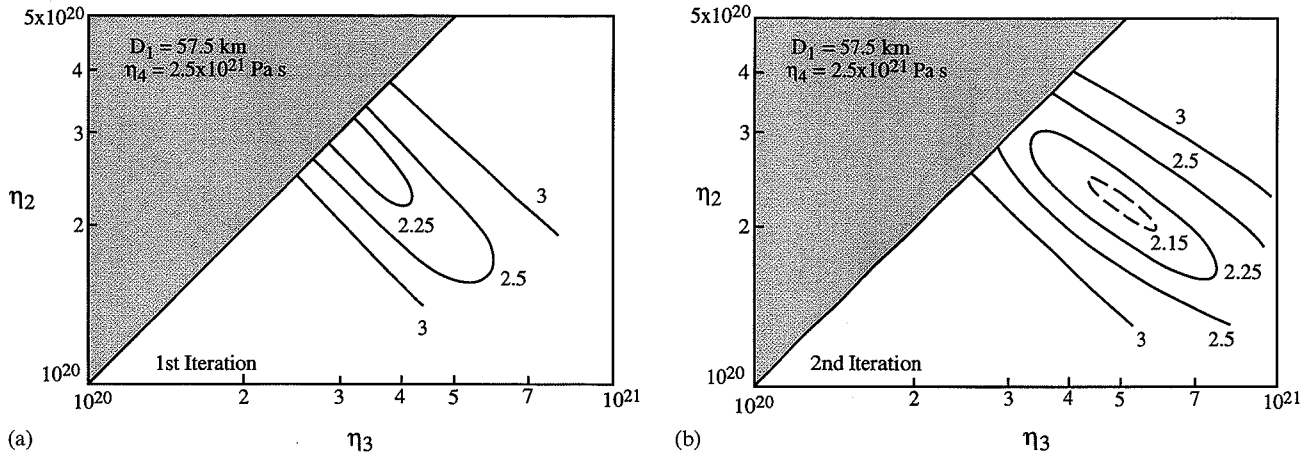

Figure 9. Minimum-variance function for the first- and second-iterations, (excluding the corrective term for the eustatic sea-level) for $\eta_{lm} = 1.3\times10^{22}$, $\eta_4 = 10^{21}$ Pa s and $D_1 = 57.5$ km.

As D_1 is increased further, η_1 increases and η_2 decreases, to the point where $\eta_1 = \eta_2$ for $D_1 = 80$ km (Fig. 7c) and the solution becomes identical to the three-layered models. This latter solution is similar to that discussed in Part II (see also Lambeck 1993c), in which the search through the range of lithospheric-thickness values was only partially complete and which, in consequence, led to the conclusion that there was no strong evidence for viscosity layering in the mantle above the 670 km discontinuity. The corresponding minimum variance for this solution is larger than that for smaller D_1 and the global minimum-variance solution for this class of models occurs for $50 > D_1 > 65$ km, with $\eta_2 \simeq (1\text{–}3)\times10^{20}$, and $\eta_3 \simeq 10^{21}$ Pa s (Table 2). The second-iteration solutions give essentially the same results for the earth-model parameters, but with a further

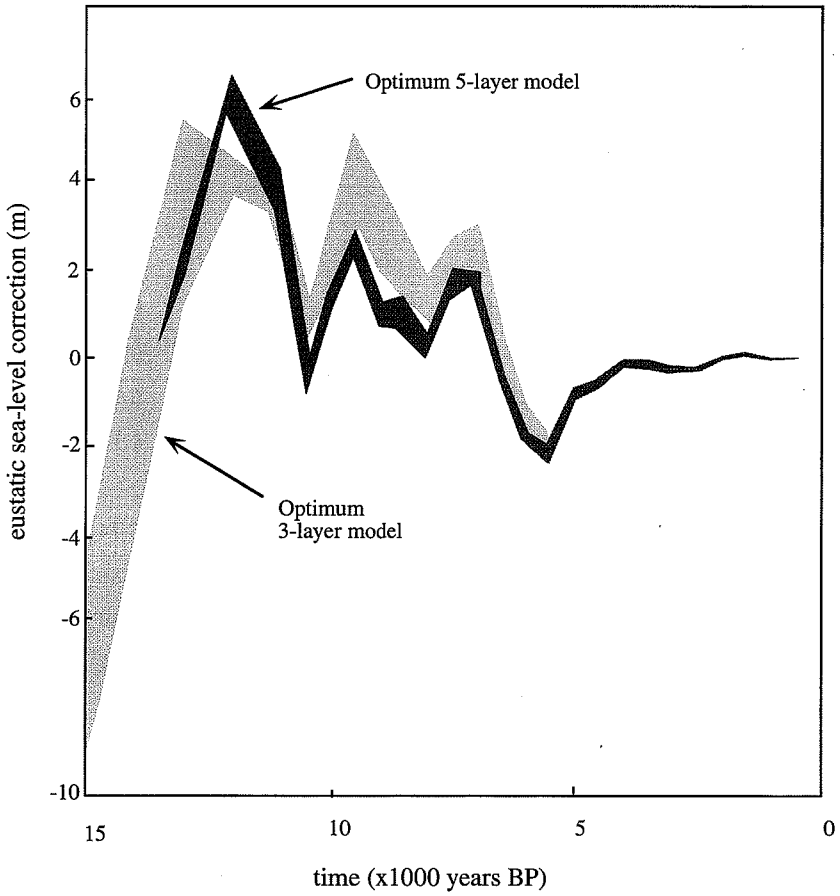

Figure 10. Range of estimates of the eustatic sea-level correction terms for the five-layered, second-iteration solutions with $D_1 = 57.5$ km corresponding to earth models in the vicinity of the minimum variance model compared with similar results for the three-layer model.

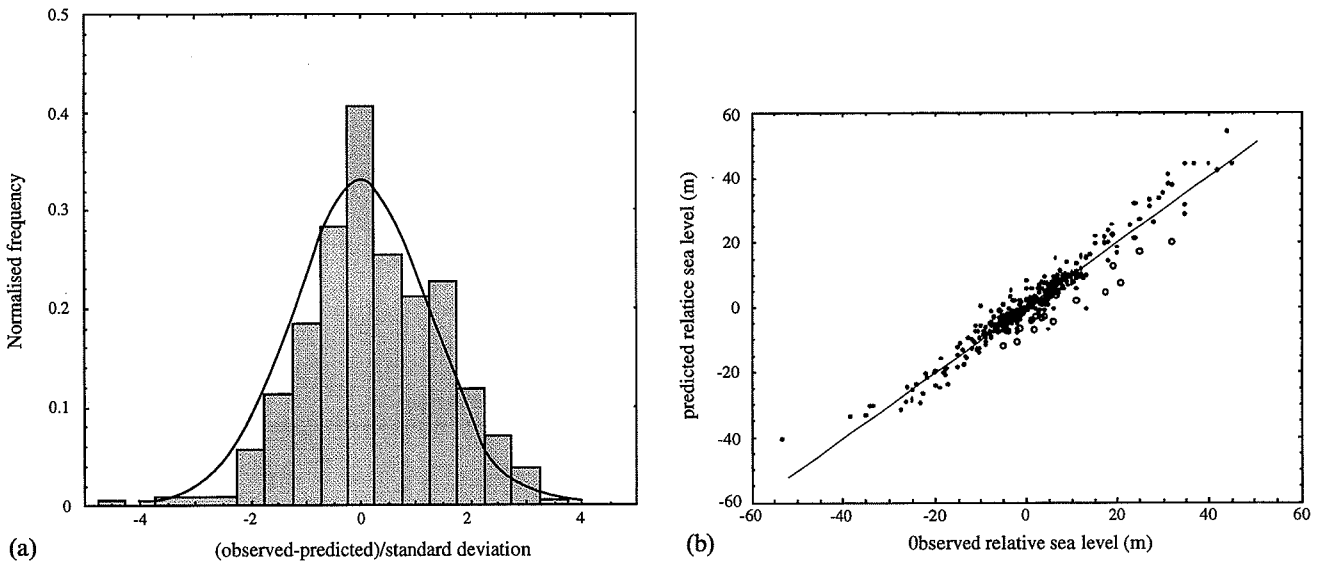

Figure 11. Statistical summary of the optimum five-layer model. (a) Histogram of residuals normalized by the standard deviations of the observations compared with the expected distribution of normally distributed data with a normalized variance of 1.4 times the assumed values for the individual observations. (b) Linear regression plot of the observed and predicted sea-levels. The open circles refer to the data points from the Beauly–Inverness area.

reduction in the overall minimum variance. The conclusion now would be that the observational data are consistent with some depth-dependent structure in the upper mantle. Similar results are obtained for a lower-mantle viscosity of 0.5×10^{22} Pa s, except that the overall variances are about 10–20 per cent greater than for the previous case (Table 2), confirming the earlier conclusion that the lower mantle has a considerably higher viscosity than the average value of the

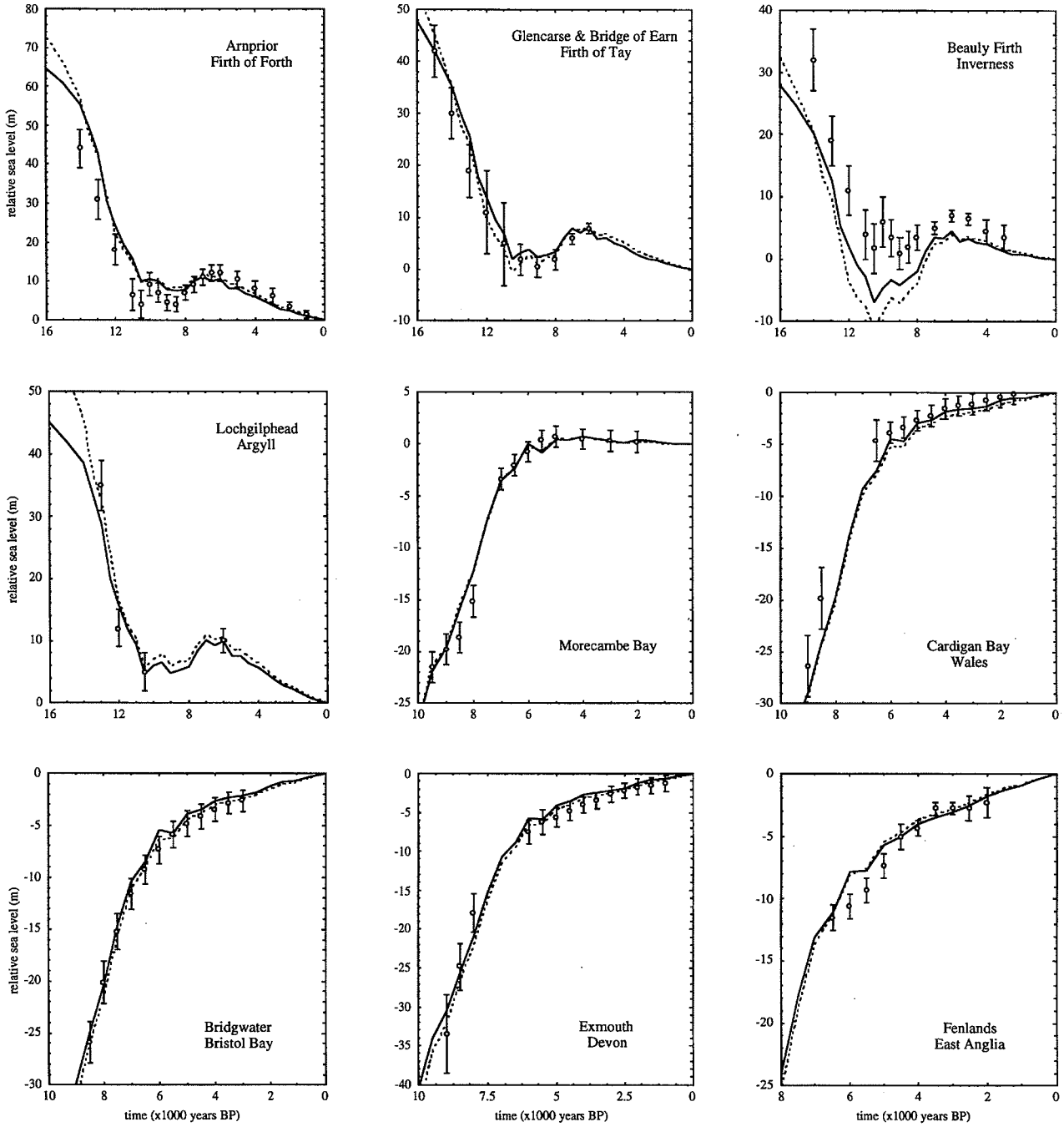

Figure 12. Comparison of observations (open circles with error bars) with predictions for selected sites using the optimum five-layer model (solid lines), and, for comparison, the optimum three-layer model (dashed lines). Both solutions include the second iteration, and eustatic corrective terms.

overlying sub-lithospheric mantle. The thin lithosphere models require quite low values for the β parameter, and the predicted maximum ice height is only of the order of 800 m.

The overall minimum variance obtained for these four-layer models is less than that for the first-iteration three-layer models (compare Figs 7 and 5(a); see also Tables 1 and 2), indicating that there may be some structure in the depth dependence of the viscosity of the upper mantle, although there appears to be no case to support the existence of a pronounced narrow, low-viscosity channel beneath a thin lithosphere. Four-layer models in which the boundary of the second layer is placed at $D_2 = 400$ km (Fig. 1) give similar results to that of the $D_2 =$ 200 km models, except that the viscosities are slightly modified and the overall minimum variance is further reduced (Table 2), arguing against much structure in the mantle viscosity above 400 km depth. Likewise, four-layer models in which D_2 is less than 200 km lead to smaller values for η_2 (Table 2), but the minimum variance is significantly greater than for any of the mantle models without the pronounced low-mantle-viscosity channel immediately below the lithosphere.

4 FIVE-LAYER MODELS

The results for the four-layer models suggest that the observational data may have some resolving power for the viscosity structure of the upper mantle, and that, because of the trade-off that occurs between the upper-mantle parameters, further exploration of the model space is warranted, particularly as the least variance is still significantly greater than unity. In the following series of models the mantle above 670 km depth is defined by the lithosphere as before, and by layers bottoming at 200, 400, and 670 km, respectively (Fig. 1). Based on the three- and four-layer-model results, the lower mantle is assumed to have an effective viscosity of $\eta_{lm} = 1.3 \times 10^{22}$ Pa s. Comparisons with earlier results based on $\eta_{lm} = 0.5 \times 10^{22}$ Pa s (Part II) confirm that the higher-viscosity value leads to a smaller overall minimum-variance factor without modifying in any significant manner the estimates for the other mantle parameters. Only models with $\eta_2 < \eta_3 < \eta_4 < \eta_{lm}$ are considered in the present calculations. Fig. 8 illustrates the first-iteration results for the case $D_1 = 65$ km, $\eta_{lm} = 1.3 \times 10^{22}$ Pa s and for discrete values of η_4, the viscosity of the transition layer between 400 and 670 km depth. For each value of η_4 illustrated in the four panels of Fig. 8 the local minimum occurs for $\eta_2 \simeq \eta_3$, and, at least for this choice of D_1, there appears to be no evidence in support of viscosity layering in the mantle between the base of the lithosphere and 400 km depth. But, as already intimated by the four-layer model results, the viscosity of the transition zone may be considerably larger than for the sub-lithospheric mantle above 400 km. Results for thick-lithosphere models are similar (Table 3) except that the minimum variance is increased. For smaller values of the lithospheric thickness a low-viscosity zone immediately beneath the lithosphere is again implied (Table 3), but such a model represents only a local minimum in the wider five-layer model space.

The second-iteration solutions result in a further reduction in the overall minimum variance, although for $D_1 = 65$ and 80 km the earth-model parameters remain essentially unchanged (Table 3). For the lower D_1 values ($D_1 = 57.5$ and 50 km), however, some shift in the η_2–η_3 parameters is noted (Fig. 9; Table 3). This apparently comes about because the characteristic spatial wavelength of the second-iteration corrections, determined mainly by the gravitational attraction of the ice sheets and by the surface deformation and the dimensions of the North Sea, is of such a magnitude that these load terms stress the upper mantle and contribute, therefore, to the separation of the mantle parameters. The introduction of the corrective equivalent sea-level term further reduces the minimum variance, to about 1.5, without any further shift in the earth-model parameters. The solution for the corrective term itself (Fig. 10) is similar to that for the three-layer models, except that the magnitude of the corrections for the earlier epochs is substantially reduced, pointing to the five-layer models' providing a better fit to the late-glacial observational data.

5 DISCUSSION

Within the range of models explored here, the model in best overall agreement with the observations is the five-layer model with the following effective parameters:

$$
\begin{aligned}
&55 < D_1 < 60 \text{ km};\\
&(2 < \eta_2 < 4) \times 10^{20} \text{ Pa s for } (D_1 < D \leq 200) \text{ km};\\
&(4 < \eta_3 < 6) \times 10^{20} \text{ Pa s for } (200 < D \leq 400) \text{ km};\\
&\eta_4 \sim 2 \times 10^{21} \text{ Pa s for } (400 < D \leq 670) \text{ km};\\
&\eta_{lm} \gtrsim 10^{22} \text{ Pa s for } (670 < D < D_{cmb}) \text{ km}.
\end{aligned}
\tag{4}
$$

This is based on the assumptions that $\eta_2 \leq \eta_3 \leq \eta_4 \leq \eta_{lm}$ and that no other minima develop with smaller overall variance beyond the explored parameter range of approximately:

$$
\begin{aligned}
&3 \times 10^{19} \geq \eta_1, \eta_2, \eta_3, \eta_4, \geq 5 \times 10^{21} \text{ Pa s};\\
&10^{21} \geq \eta_{lm} \geq 10^{23} \text{ Pa s};\\
&30 \geq D_1 \geq 120 \text{ km}.
\end{aligned}
$$

The above estimates (4) are effective parameters in the sense that they describe the response of the planet to surface loading well on time-scales of the order of 10^4 a, with stress differences of the order of 10 MPa, and based on the assumption of a Maxwell viscoelastic rheology. Models with a viscosity inversion, other than at the base of the lithosphere, have not at present been examined. Models with, for example, a viscosity varying more smoothly with depth may also fit the observational sea-level data equally well, but such models have not been examined. The results indicate that there is no compelling case for a strong increase in the mantle viscosity between the base of the lithosphere and the 400 km seismic discontinuity and that a narrow low-viscosity channel immediately below the lithosphere is not required. But the solutions do point to a substantial increase in the viscosity, by a factor of three or four between this upper-mantle region and the transition zone. A further increase of viscosity by an order of magnitude appears to be required across the 670 km boundary. The resolving power of this data for the viscosity of the lower mantle is poor, and no attempt has been made to establish whether depth dependence of viscosity occurs below 670 km. The surface response to the loading of the larger ice sheets may, however, help to resolve the question of viscosity structure in this region, as well as improving upon the resolution of the structure above 670 km.

With the exception of the possible zonation between the base of the lithosphere and 400 km depth, the above features of the mantle rheology appear to be robust and independent of details of the solutions, such as whether the second-iteration terms are included or not, although the inclusion of these terms does improve the overall fit of the model to the data. Also, as discussed in Part II and in Lambeck (1993c), the solutions for the earth-model parameters, based on surface loads of relatively small extent, appear to be independent of the assumptions made about the nature of the response to loading of the phase transformation boundaries at 400 and 670 km. The present models assume that the kinetics of the phase transformations are slow enough such that they do not occur on the time-scales considered here, and that density contrasts across these boundaries are advected with the flow, but models with rapid phase-transformation kinetics do not yield very different results for the Great Britain loading problem, other than a modification of the ice-scaling parameter, β, which is reduced by about 10 per cent. Thus, for this scale of ice load at least, and provided that the ice-scaling parameter is introduced, the assumption of no exchange of mass across the boundaries is adequate (see also Johnston, Lambeck & Wolf 1996).

The results for the multi-layered models illustrate the trade-

offs that can occur between the various parameters that define the Earth's response. They also illustrate the consequences of not searching through a complete range of plausible model space, although the expanded search does incur the cost of very substantial computing time. If, as done by Fjeldskaar (1994), the lithospheric thickness is fixed at a relatively low value ($\gtrsim 50$ km) then the solution points to a low-viscosity channel beneath the lithosphere, a result that is reinforced if the thickness of this channel is also reduced, such as the four-layer model with $D_2 = 150$ km (Table 2). But these solutions represent local minima only, and more solutions covering a wider parameter space do not support such results, at least not for the Great Britain region. Likewise, the imposition of a thick lithosphere on the viscosity structure, without conducting a full search of the model space, leads to a local minimum solution that does not correspond to the global minimum variance. Thus, an adoption of a relatively thick lithosphere, of say 100–120 km, as used in the recent models of Peltier and colleagues (Mitrovica & Peltier 1993; Tushingham & Peltier 1992), leads to an overestimation of the upper-mantle viscosity and to models in which the contrast between upper- and lower-mantle viscosity is much less than that found here (see e.g. Fig. 2c). However, such solutions represent only local minima within a larger earth-model parameter domain.

If independent information on the appropriate choice for lithospheric thickness were available then this would significantly improve the solutions for the viscosity profile because it would eliminate some of the correlations that otherwise occur between the various parameters. Through the representation of the lithosphere as a simple elastic layer, its effective thickness will be dependent on the duration of loading because of the tendency for the load stresses within this layer to migrate with time from the weaker zones into the stronger zones. Thus, seismic data will generally give relatively large values for D_1, whereas estimates based on tectonic studies with characteristic loading time-scales of 10^6 to 10^7 a will usually lead to lower values. The glacial-rebound estimates, appropriate for the response to loading on time-scales of the order of 10^3 to 10^5 a, are expected to fall between these limits, but exactly where depends on the stress-relaxation processes in the layer. Realistic *a priori* assumptions about the lithospheric thickness cannot be made for this problem, and the estimation of this parameter from the glacial-rebound studies is, in fact, an important element in reaching an understanding of the lithospheric response to loading over a wide range of load cycles.

One consequence of the trade-off between the earth-model parameters is that it is not permissible to mix models, as has sometimes been done. For example, Fjeldskaar & Cathles (1992) combined a set of mantle-viscosity parameters of Lambeck *et al.* (1990), corresponding to a thick-lithosphere ($D_1 = 200$) model (which the latter rejected on the grounds that it produced an excessively large correction to the eustatic sea-level), with their own thin-lithosphere model to argue that the former viscosity parameters do not lead to a satisfactory estimate of present changes in sea-level for the Scandinavia area. But these viscosity parameters are only valid if used with the corresponding D_1 value, and, if the requirement of internal consistency of model parameters is maintained, the model does lead to reasonable predictions of the glacio-hydro isostatic contribution to present sea-level change [see, for example, the predicted contributions to present sea-level for Great Britain and the North Sea in Lambeck (1993d, e) for earth models with $D_1 = 65$ km and no low-viscosity channel]. The trade-off between ice- and earth-model parameters may also have important consequences. Clearly, any ice-model parameters inferred from relative sea-level observations will be a function of the adopted earth-model parameters. A model with a thick lithosphere will, for example, lead to an increase in ice volume in such an inference, but the solution will not represent a global minimum unless a complete search through both ice- and earth-model parameter space is carried out.

As already noted in Part II the optimum three-layer model describes the characteristic patterns of the sea-level change observed around the British Isles well and gives results that are very similar to the optimum five-layer model for most of the sites. Thus the former model is largely adequate for exercises such as predicting shoreline evolution or estimating ice heights. Fig. 11 illustrates some of the statistics of the comparison of the optimum five-layer solution with the observational data. The histogram of the residuals, the observed minus the predicted sea-levels normalized by the observational standard deviations, is illustrated in Fig. 11(a). The residuals are consistent with normally distributed observational errors with standard deviations that may be about 20 per cent greater than the assumed values. The plot of observed versus predicted sea-levels confirms the generally good agreement, with a linear regression coefficient of 1.00. The small group of outliers (open circles in Fig. 11b), falling below the linear regression line, corresponds mainly to observations from the Beauly and Inverness Firths where the model systematically underestimates the rebound. This is typified by the Beauly result illustrated in Fig. 12, and it has previously been concluded, from observations in this region, as well as from data from north-western Scotland, that this points to a deficiency in the ice load over northern Scotland, north of the Great Glen, at the time of the last glacial maximum (Part II; Lambeck 1995a,b). Comparisons of predictions and observations for some of the other sites are also illustrated in Fig. 12, and these, also, point to a generally good agreement between the two.

Tests with the present ice model, as well as with a modified ice model, in which the ice thickness over northernmost Scotland has been increased (see Part II, Section 5), have shown that the limitation of the ice model used in the above analyses does not modify the mantle parameters in any significant way, provided that the overall scale factor β^{GB} is introduced as an unknown. The modified ice model, with increased ice over northern Scotland, does lead to a further variance reduction, and for the optimum five-layer model parameters, including the far-field correction, this is reduced to 1.35 (Table 3). Important new observational data for this region are now being collected by I. Shennan and colleagues, and this should provide important constraints in future modelling of the ice sheet.

ACKNOWLEDGMENTS

This research has been partly funded by the Ministerie van Verkeer en Waterstaat, Directoraat-Generaal Rijkwaterstaat, the Netherlands.

REFERENCES

Boulton, G.S., Smith, G.D. & Morland, L.W., 1984. The reconstruction of former ice sheets and their mass balance characteristics using a non-linearly viscous flow model, *J. Glac.*, **30**, 140–152.

Boulton, G.S., Smith, G.D., Jones, A.S. & Newsome, J., 1985. Glacial geology and glaciology of the last mid-latitude ice sheets, *J. geol. Soc. Lond.*, **142,** 447–474.

Cathles, L.M., 1975. *The Viscosity of the Earth's Mantle,* Princeton University Press, Princeton, NJ.

Daly, R.A., 1934. *The Changing World of the Ice Age,* Yale University Press, New Haven, CI.

Dziewonski, A.M. & Anderson, D.L., 1981. Preliminary reference Earth model, *Phys. Earth planet. Inter.*, **25,** 297–356.

Fjeldskaar, W., 1994. Viscosity and thickness of the asthenosphere detected from the Fennoscandian uplift, *Earth planet. Sci. Lett.*, **126,** 399–410.

Fjeldskaar, W. & Cathles, L., 1992. The present rate of uplift of Fennoscandia implies a low viscosity asthenosphere, *Terra Nova,* **3,** 393–400.

Johnston, P., 1993. The effect of spatially non-uniform water loads on the prediction of sea-level change, *Geophys. J. Int.*, **114,** 615–634.

Johnston P., Lambeck, K. & Wolf, D., 1996. Material versus isobaric internal boundaries in the Earth and their influence on glacial rebound, *Geophys. J. Int.*, in press.

Lambeck, K., 1993a. Glacial rebound of the British Isles—I. Preliminary model results, *Geophys. J. Int.*, **115,** 941–959.

Lambeck, K., 1993b. Glacial rebound of the British Isles—II. A high resolution, high-precision model, *Geophys. J. Int.*, **115,** 960–990.

Lambeck, K., 1993c. Glacial rebound and sea-level change: an example of a relationship between mantle and surface processes, *Tectonophysics,* **223,** 15–37.

Lambeck, K., 1993d. Glacial rebound of the British Isles, sea-level change and shoreline evolution, in *Late Quaternary and future sea-level changes in the eastern Irish Sea area, British Geological Survey Workshop Report WB/93/23R,* pp. 4–16, Keyworth.

Lambeck, K., 1993e. Sea level, ice sheets, and the physics of the Earth, *Kon. Ned. Akad. Wetensch,* **102,** 76–81.

Lambeck, K., 1995a. Late Devensian and Holocene shorelines of the British Isles and North Sea from models of glacio-hydro-isostatic rebound, *J. geol. Soc. London,* **152,** 437–448.

Lambeck, K., 1995b. Glacial isostasy and water depths in the Late Devensian and Holocene on the Scottish shelf west of the Outer Hebrides, *J. quat. Sci.*, **10,** 83–86.

Lambeck, K. & Nakada, M., 1990. Late Pleistocene and Holocene sea-level change along the Australian coast, *Palaeogeog. Palaeoclimat., Palaeoecol.*, **89,** 143–176.

Lambeck, K., Johnston, P. & Nakada, M., 1990. Holocene glacial rebound and sea-level change in NW Europe, *Geophys. J. Int.*, **103,** 451–468.

Mitrovica, J.X. & Peltier, W.R., 1993. The inference of mantle viscosity from an inversion of the Fennoscandian relaxation spectrum, *Geophys. J. Int.*, **114,** 45–62.

Mitrovica, J.X., Davis, J.L. & Johansson, J.M., 1995. The radial profile of mantle viscosity: searching for a consensus, *Int. Un. Geod. Geophys. General Assembly, Boulder,* p. B395, (abstract).

Nakada, M. & Lambeck, K., 1988. The melting history of the Late Pleistocene Antarctic ice sheet, *Nature,* **333,** 36–40.

Nakada, M. & Lambeck, K., 1989. Late Pleistocene and Holocene sea-level change in the Australian region and mantle rheology, *Geophys. J.*, **96,** 497–517.

Peltier, W.R., 1984. The thickness of the continental lithosphere, *J. geophys. Res.*, **89,** 11 303–11 316

Peltier, W.R., 1986. Deglaciation-induced vertical motion of the North American continent and transient lower-mantle rheology, *J. geophys. Res.*, **91,** 9099–9123.

Peltier, W.R. & Tushingham, A.M., 1991. The influence of glacial isostatic adjustment on tide gauge measurements of secular sea level change, *J. geophys. Res.*, **96,** 6679–6696.

Peltier, W.R., Drummond, R.A. & Tushingham, A.M., 1986. Postglacial rebound and transient lower-mantle rheology, *Geophys. J. R. astr. Soc.*, **87,** 79–116.

Tushingham, A.M. & Peltier, R.W., 1992. Validation of the ICE-3G Model of Wurm-Wisconsin Deglaciation using a global data base of relative sea level histories, *J. geophys. Res.*, **97,** 3285–3304.

van Bemmelen, R.W. & Berlage, H.P., 1935. Versuch Einer Mathematischen Behandlung Geotektonischer Bewegungen unter Besonderer Berucksichtegung der Undationstheorie, *Gerlands Beitr. Geophys.*, **42,** 19–55.

Wolf, D., 1993. The changing role of the lithosphere in models of glacial isostasy: a historical review, *Global Planet. Change,* **8,** 95–106